CFD SIMULATION AND MEASUREMENT OF THE HEAT TRANSFER FROM BUILDING MATERIAL SPECIMENS TO THE INDOOR ENVIRONMENT

Conrad Voelker[1], Markus Diewald[2]
[1]Bauhaus-University Weimar
[2]University of Kaiserslautern

ABSTRACT

During concrete endurance and fatigue tests with a high frequency of load changes, the investigated building material specimens can become very hot. To investigate the heat generation as well as the heat transfer to the indoor environment, an experimental setup was erected. A special feature of the setup was an embedded heating coil which controlled the temperature of the specimen. Temperature sensors measured the surface as well as the core temperature of the specimen. Additionally, the air temperature and flow field surrounding the probe was measured using thermistors and anemometry. To visualize the temperature profile of the specimen's micro-climate, infrared thermography was used. Because thermography detects only surface temperatures, but not air temperature, an auxiliary work plane made of cardboard was built around the specimen. This allowed us to visualize the corona-shaped boundary layer of the specimen and allowed the temperature to be measured throughout the whole plane, not only at the individual points where the thermistors were located.

The measurements were complemented with simulations using computational fluid dynamics (CFD). Using a coupled CFD simulation, the heat transfer within the specimen (conduction) and the heat transfer to the indoor environment (convection, radiation) were simulated. In the simulations, different boundary conditions have been studied. For the validation of the CFD simulations, the results have been compared with the measurements. In conclusion, the values of the simulations match the experiments quite well.

INTRODUCTION

The study of concrete fatigue under dynamic loading is relatively new but has been coming increasingly into focus in recent years. In order to investigate the fatigue behavior of such highly dynamically stressed structures, laboratory experiments must be performed which induce high numbers of load cycles ($>10^7$). High frequencies (e.g., f=50Hz) are also necessary in order to induce such a high number of load cycles quickly enough that an experiment to be completed in a timely fashion (Schneider et al., 2012). In these experiments, the specimens become extremely hot due to the transformation of the added conducted load into heat energy. The main cause of this heat generation is probably internal friction within the concrete test specimens.

The height and the distribution of the temperatures reached in these experiments have not been examined in detail so far. This includes the heat transfer from the building material specimen to the indoor environment. What also remains unknown is the possibly resulting impact of the high temperatures on the specimen. Experiments to determine the effects of concrete temperature on its mechanical material properties have been conducted, often to understand its behavior in the case of fire. These show that commonly cited material characteristics such as compressive strength, elastic modulus as well as heat conductivity and capacity are highly influenced by temperature (Hildenbrand, 1978, Collet et al., 1976) (Schneider, 1982, Phan et al., 2003).

It can thus be concluded that previous fatigue findings in which specimens reached high temperatures are highly restricted in their transferability to real-world practice. For this reason, studies on heat generation and heat transfer to the indoor environment are necessary to better estimate the temperature behavior of such specimens. The necessary prerequisite investigations for this are presented in this paper.

SIMULATION

Numerical methods

To investigate the heat transfer from the building material specimen to the indoor environment, numerical simulations as well as measurements (see next chapter) have been conducted. For the simulation, the geometric coordinates of the experimental setup were entered into the CFD software FLUENT using ICEM. In Figure 1, a screenshot of this simplified box with a volume of 1x1x2m³ is shown. The concrete specimen (UHPC – Ultra High Performance Concrete) is in the horizontal centre of the box, surrounded by the two pressure plates.

The discretization of the three-dimensional object was done using tetrahedral cells (Figure 2). The grid surrounding the specimen had to be discretized more detailed due to the heat transfer solid-fluid and high

temperature and velocity gradients. The surface-to-surface radiation model (S2S) provided by FLUENT was used. This model calculates the energy exchange in an enclosure of gray-diffuse surfaces. The radiation exchange between two surfaces depends on several parameters, which are accounted for by view factors. Additionally, FLUENT's "enhanced wall treatment" was used to for the near-wall modelling. It combines the conventional two-layer model with enhanced wall functions. All simulations were run *steady*. The numerical methods and boundary conditions of the simulation are provided in Table 1.

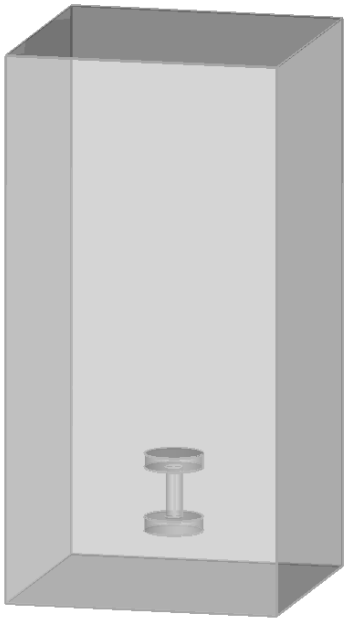

Figure 1: Geometry of the simulated specimen

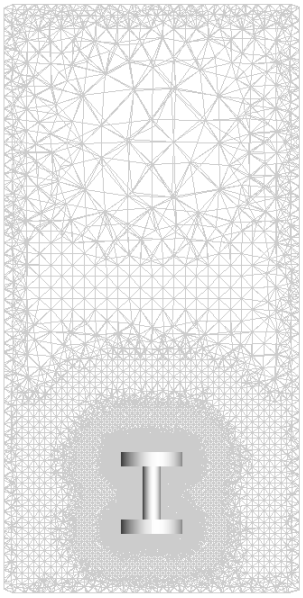

Figure 2: Mesh with local refinement surrounding the specimen

CFD results

The air temperature and flow velocity of the heat release of the specimen were simulated for various boundary conditions. In Figures 9 and 10, the results are visualized for the case of P=43W. Due to the heat release via convection, the micro-climate shows temperatures in-between the room air temperature and the surface temperature of the specimen. This temperature gradient is responsible for a density gradient, which is the reason for the air flow. This results in an ascending plume with v_{air} up to 0.3m/s.

Table 1: Geometry and numerical methods

Geometry	heating element	steel	Ø=6.5mm, h=160mm
	specimen	concrete	Ø=60mm, h=180mm
	pressure plates	steel	Ø=200mm, h=50mm
	bounding box	air	1000x1000x2000mm³
Model	ANSYS Fluent 15.0 Viscous model realizable k-ε with standard properties Enhanced wall treatment Radiation model S2S (Surface to Surface)		
Solver	Pressure-based, time steady		
Fluid	Air (standard properties, incompressible ideal)		
Solids	UHPC:	density 2500 kg/m³ specific heat capacity 1100 J/(kg K) thermal conductivity 2.4 W/(m K)	
	Steel:	density 8030 kg/m³ specific heat capacity 502.48 J/(kg K) thermal conductivity 16.27 W/(m K)	
Cell Zone Conditions	Heating element: energy source		
Boundary Conditions	Sides/Top:	pressure-outlet, no gauge pressure, backflow total temperature 293.15 K	
	Bottom:	wall with heat flux 0 W/m²	
	Steel:	coupled	
	Concrete:	coupled	
Mesh	1,500,000 tetrahedral cells 170,000 wedge cells 350,000 nodes		

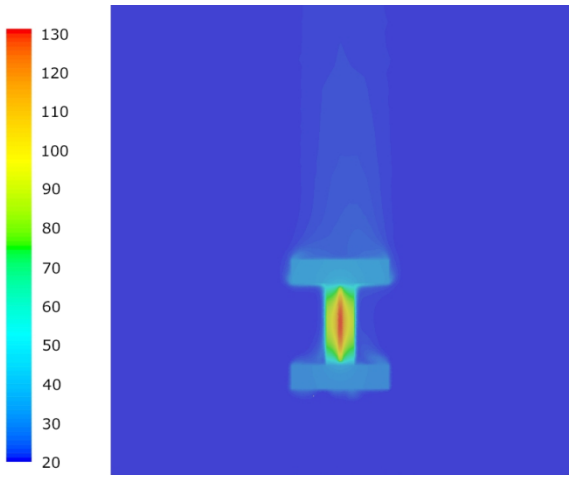

Figure 3: Simulated air temperature in the micro-climate (in °C, at P=43 W, symmetry plane through the centre)

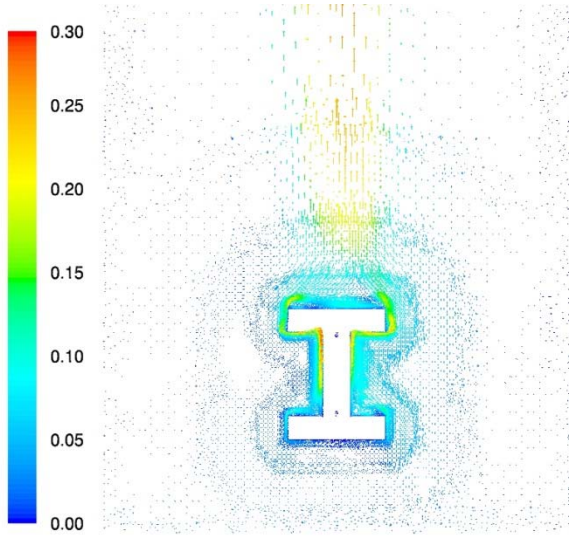

Figure 4: Simulated air velocity in the micro-climate (in m/s, at P=43 W, symmetry plane through the centre)

MEASUREMENTS

Experimental setup

A simple test model was constructed, as shown in Figure 5. The central component of this model was a cylinder made of high-performance concrete (grade C100/115), which was provided by the University of Hannover. This was placed between two steel blocks as in a conventional fatigue tester. The steel blocks were composed of two 50mm thick plates, each with a diameter of 210mm. The plates and the cylinder were not attached to each other but were simply stacked. In order to simulate the heating of the concrete, a controllable heating element was built into the concrete cylinder.

To measure the surface temperature, five evenly spaced PT100 sensors were attached to the concrete cylinder and one sensor was fixed to the edge of each of the steel plates. In addition, a thermocouple at the base of the heating element read the temperature inside the concrete core.

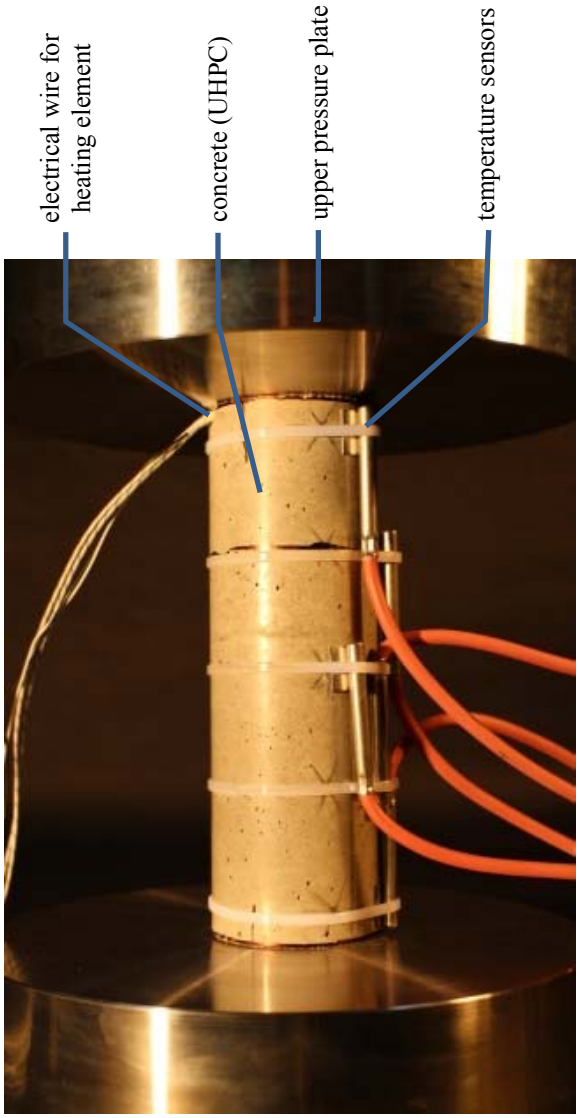

Figure 5: Structure of the model

The thermal energy given off by the heated specimen results in a transition zone (micro-climate), which is to be differentiated in temperature and flow from the surrounding climate of the room. To measure the transition zone, further temperature and flow sensors were installed. NTC sensors were mounted above the experimental setup to measure the air temperature (Figure 6) and a hot-wire anemometer was fixed to the experimental setup to measure flow rate. Measurements of the air temperature and flow were conducted at separate times to avoid interference by the heat output of the anemometer. In our preliminary experiments it was found that the heat emitted by the hot-wire anemometers influenced the air temperature. Therefore, air temperature and flow velocity were subsequently measured separately. Finally, a temperature sensor for measuring the ambient temperature was placed next to the experiment setup.

The only parameter that was changed in the different experiments was the output of the heating element (Table 2).

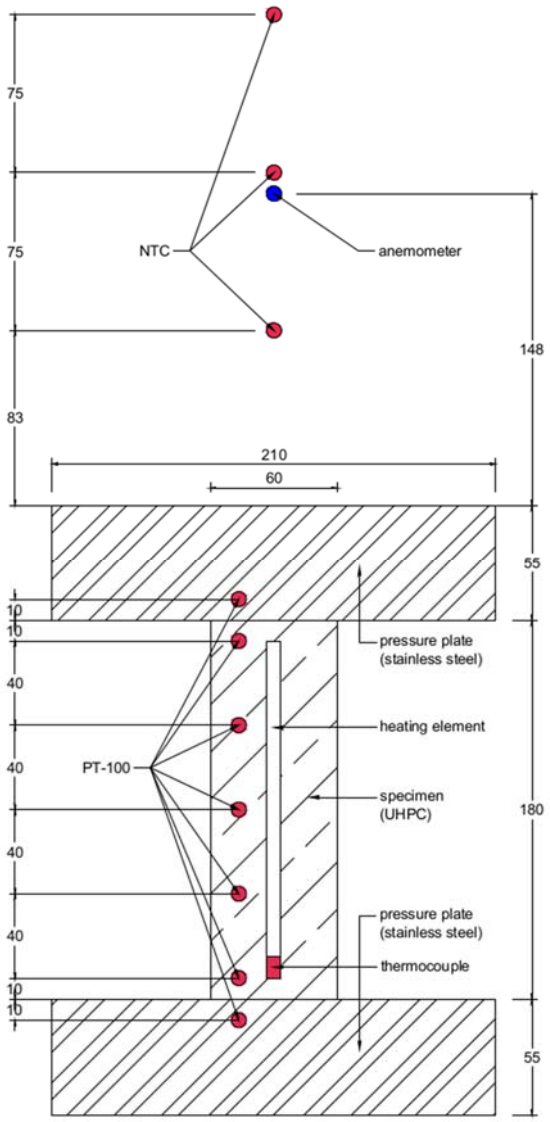

Figure 6: Vertical section of the measurement setup

Table 2: Measuring program

NO.	POWER [W]
1	3
2	6
3	10
4	15
5	20
6	31
7	43
8	54

Temperature and air flow

Before starting the actual measurements, the thermal steady state had to be reached. Figure 7 shows an example, with the case P=43W, where the warm-up phase is shown. The time needed to reach steady state is long (several hours), but short in comparison to the duration of real fatigue tests (several weeks). After the system had reached a relatively steady state, the actual measurements were started. During the recordings, fluctuations are always present, especially of the flow velocity. These fluctuations are mainly attributable to air flow turbulence and instability. Therefore, measurements were recorded over a time period of t=1h with a sampling interval of t=1s and then averaged. This makes the anemometry measurements comparable to the results of the statistically averaged CFD simulation based on Reynolds-Averaged-Navier-Stokes equations (RANS). The results of all measurements are summarized in Figure 8.

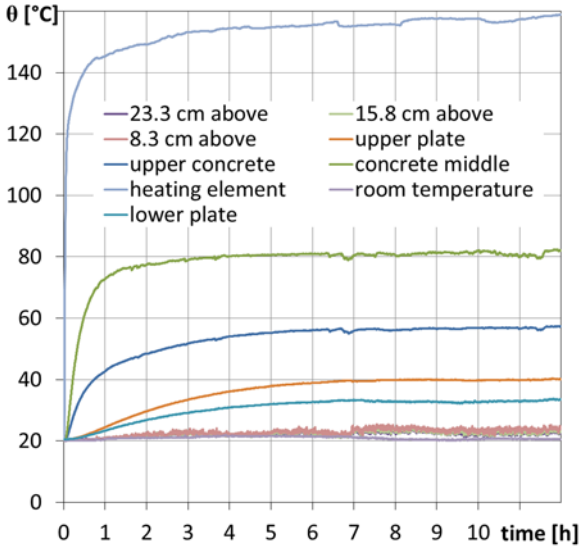

Figure 7: Heating until reaching steady-state (P=43 W)

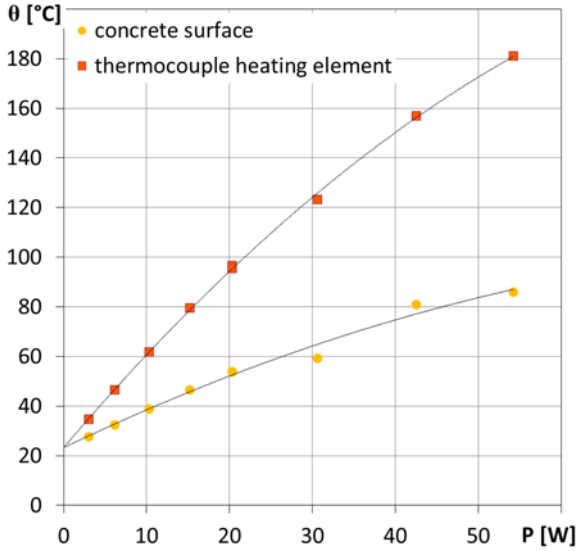

Figure 8: Temperature of the heating element (thermocouple) and concrete surface (middle PT-100) after reaching steady-state

Thermography

To visualize the air temperature profile of the specimen's micro-climate, infrared thermography was used as previously documented (Voelker et al., 2014). Because thermography detects only surface temperatures, but not air temperature, an auxiliary work plane made of cardboard (thickness ~0.5mm) was built around the specimen. The surface temperature of the auxiliary work plane was measured with the infrared Jenoptik Varioscan 3021 camera with LN2 cooling. The camera has a resolution of ±0.03 K, so that temperature gradients can be represented quite accurately in a single thermogram.

During the experiment, it was again necessary to wait until the system had reached a thermal steady state, where the surface temperature of the auxiliary work plane was nearly the same as the air temperature. This state could be reached quickly because the thin cardboard has a very low heat capacity. When the cardboard plane was mounted, care was taken to avoid direct contact with the surface of the setup in order to reduce heat conduction effects orthogonal to the specimen.

Finally, the use of infrared thermography allowed us to visualize the corona-shaped boundary layer of the setup (Figure 9). Hence, the temperature was measured throughout the whole plane, not only at the individual points where the thermistors were located.

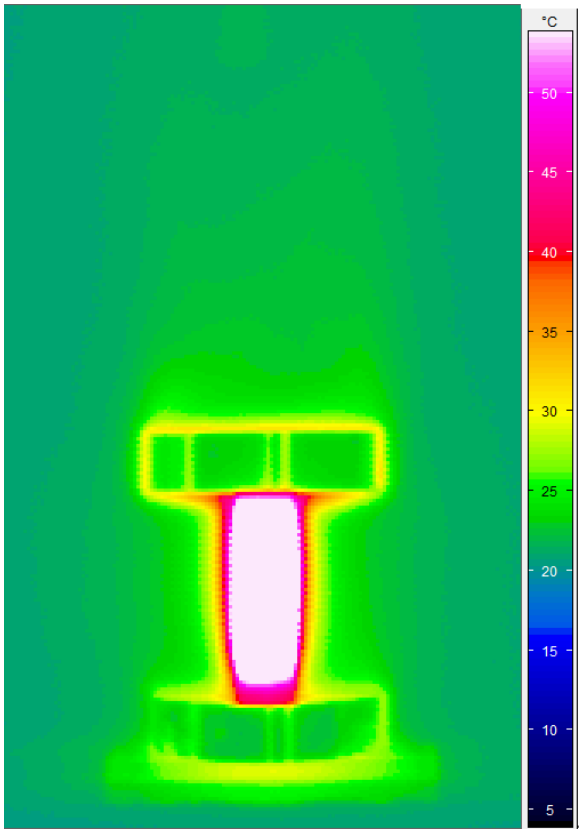

Figure 9: Thermography of the work plane (P=43W), visualizing the temperature of the micro-climate

To validate the CFD simulation, the results were compared with the measurements. Figure 10 compares the simulated and the measured temperatures of air and specimen. The four values in the case of the air temperature in particular show very good agreement as do those of the steel plates. Only the simulated concrete temperatures deviate from the measurements. Also imperfectly simulated is the flow velocity: the simulated air flow is twice as fast as the measurement. The absolute deviation is small (Δv=0.1m/s), but the relative deviation is rather large. The error bar of the measured flow velocity expresses the standard deviation, which is quite high due to the fluctuations resulting from turbulence and instability of the flow. The error bars describing the standard deviation of the temperatures are not visible because it is so little.

In summary, a good agreement with the simulation could be found, when taking into account errors in measurement. Minor inaccuracies were due to the fact that both measurement and simulation are only an approximation of reality.

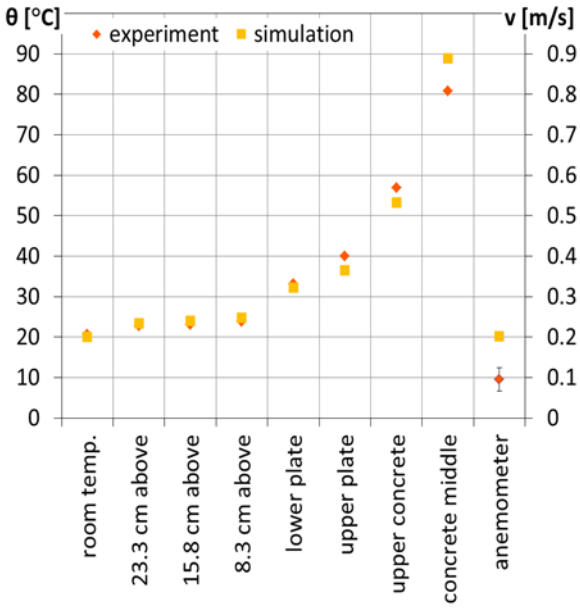

Figure 10: Comparison of simulation & measurement

CONCLUSION

To investigate the heat transfer of concrete specimen to the indoor environment, an experimental setup was constructed. The measurements showed good agreement with CFD simulations. Both measurements and simulations showed that the concrete temperatures depend on their supplied energy. However, the heat transfer also depends on the geometry of the specimen and the fatigue tester as well as on boundary conditions. Further study is

planned to determine the exact nature of these influencing factors.

ACKNOWLEDGMENTS

We appreciate the cooperation with the Universität Hannover, Institut für Massivbau, Prof. Dr.-Ing. Steffen Marx & Dipl.-Ing. Sebastian Schneider. We thank Daniel Schwab for his support.

REFERENCES

Collet, Y.Tavernier, E. 1976. Etude des propiétés du béton soumis á des températures élevées, Groupe de Travail, Comportement du Matériau Béton en Fonction de la Température.

Hildenbrand, G. 1978. Untersuchung der Wechselwirkung von Kernschmelze und Reaktorbeton, Abschlussbericht Forschungsvorhaben BMFT RS 154, Erlangen.

Phan, L.T.Carino, N.J. 2003. Code provisions for high strength concrete strength-temperature relationship at elevated temperatures, Materials and Structures, 36, 91-98.

Schneider, S., Vöcker, D.Marx, S. 2012. Zum Einfluss der Belastungsfrequenz und der Spannungsgeschwindigkeit auf die Ermüdungsfestigkeit von Beton, Beton- und Stahlbetonbau, 107, 836–845.

Schneider, U. (1982) Verhalten von Beton bei hohen Temperaturen, Berlin, Beuth Verlag.

Voelker, C., Maempel, S., Kornadt, O. 2014. Measuring the human body's micro-climate using a thermal manikin, Indoor Air, 24, 567–579.